PCCP

PERSPECTIVE

View Article Online
View Journal | View Issue

Cite this: *Phys. Chem. Chem. Phys.*, 2019, **21**, 11554

Exploring membrane organization at varying spatiotemporal resolutions utilizing fluorescence-based approaches: implications in membrane biology

Parijat Sarkar and Amitabha Chattopadhyay *

Received 13th April 2019,
Accepted 21st May 2019

DOI: 10.1039/c9cp02087j

rsc.li/pccp

Biological membranes are characterized by lateral inhomogeneities, termed as membrane domains, which are regions enriched with specific types of lipids and proteins. While the functional consequences of membrane domains are well understood, the physicochemical study of domains has proved to be elusive, mainly due to varying spatiotemporal scales associated with them. In this perspective, we provide an overview of representative experimental approaches based on dynamic fluorescence microscopy to analyze organization and dynamics of membrane lipids and proteins. We further elucidate variation of dynamics as a function of area of observation, a unique feature of biological membranes, and its modulation with membrane components such as cholesterol and the actin cytoskeleton. In terms of spatial resolution, we provide examples from super resolution techniques that overcome the diffraction limit encountered in conventional optical microscopes. We conclude that judicious use of a combination of approaches of varying spatiotemporal resolutions, commensurate with spatiotemporal scales of a given membrane process, would provide a comprehensive dynamic model of the biological membrane in terms of membrane organization, dynamics and function.

1. Biological membranes and membrane receptors

Biological membranes are complex two-dimensional, micro-heterogeneous, non-covalent assemblies of a diverse variety of lipids and proteins.[1] Our current understanding of the organization and dynamics of biological membranes involves the concept of lateral heterogeneities, collectively termed as 'membrane domains'.[2,3] These specialized areas are believed to be enriched in specific lipids and proteins and facilitate processes such as ion transport, trafficking, sorting and signal transduction over a range of spatiotemporal scale (see Fig. 1). The eukaryotic plasma membrane exhibits a rather complex architecture in terms of organization of membrane components and represents the first platform where cellular signaling is initiated.[5] The organizational complexity of the membrane, as revealed by a variety of approaches, strongly depends on the spatiotemporal scale associated with the chosen approach. A comprehensive picture of the cell membrane would therefore emerge from simultaneous mapping of membrane heterogeneity at various spatial and temporal scales.

The majority of functions in biological membranes are carried out by membrane proteins. G protein-coupled receptors (GPCRs) are the largest class of intrinsic membrane proteins that transduce various extracellular stimuli by triggering intracellular signaling through coupling with effector proteins.[6–9] GPCRs are polytopic proteins and consist of seven α-helical transmembrane passes. They include >800 members that are encoded by ~5% of the human genome.[10] GPCRs signal in response to binding of a wide range of ligands and act as highly versatile and dynamic signaling hubs in the membrane.[11,12] They mediate a plethora of cellular responses to a diverse variety of stimuli in numerous physiological processes. As a consequence of the wide range of signaling pathways regulated by GPCRs, these receptors have been at the forefront of drug development efforts in all clinical areas.[9,13–15] In fact, ~40% of all current drug targets are GPCRs.[16–18]

2. The relevance of spatiotemporal scale in appreciating membrane dynamics

A remarkable characteristic of biological membranes is their inherent dynamics that spans over a wide spatiotemporal scale (see Fig. 1).[1,4,19,20] Segmental (domain) motion in a protein takes place at the sub-μs time scale, whereas local dynamics (fluctuations) occur at sub-ns to sub-μs time scale. Most biological

CSIR-Centre for Cellular and Molecular Biology, Uppal Road, Hyderabad 500 007, India. E-mail: amit@ccmb.res.in; Tel: +91-40-2719-2578

processes carried out by the major classes of transmembrane proteins (*e.g.*, ion transport across channels, signal transduction by GPCRs) occur at a much slower time scale (ms–s or longer). Lateral diffusion of membrane proteins and lipids display long-range dynamics ($\sim\mu$m), with lipid diffusion an order of magnitude faster than membrane protein diffusion. Study of organization and dynamics of membranes therefore demands the use of diverse experimental techniques with a wide window of spatiotemporal sensitivity. Due to this reason, while some experimental techniques generate a stationary (static) snapshot of membranes (since the measurement time scale of the technique is fast relative to molecular motion), other approaches would portray a time-averaged picture of a fast moving molecule with respect to the measurement time scale. In this context, experimental methods based on fluorescence spectroscopy offer a suitable approach and are widely used to measure various membrane phenomena across a wide range of spatiotemporal scales. These methods include fluorescence correlation spectroscopy (FCS), fluorescence resonance energy transfer (FRET), fluorescence recovery after photobleaching (FRAP), and wavelength-selective fluorescence approach.[21–27] Fluorescence-based techniques offer certain advantages due to their superior sensitivity, minimal perturbation to the native system and a host of measurable parameters, that help the study of several membrane associated processes. In this review, we will provide a brief outline of representative experimental approaches based on dynamic fluorescence microscopy to analyze membrane lipid and protein dynamics, along with super resolution techniques capable of beating the diffraction limit of conventional optical microscopes. We believe that judicious use of experimental approaches, compatible with spatiotemporal scales of the given membrane process, would provide a comprehensive dynamic model of the biological membrane.

3. Membrane dynamics: the importance of lateral diffusion

A major motivation behind studying membrane dynamics is the fact that understanding of lipid and protein dynamics provides novel insights in cellular function. The conformational flexibility of membrane proteins in a dynamic and fluid membrane milieu in the context of their function constitutes an emerging area of research.[28–30] Work from our and other groups has shown that receptors such as GPCRs exhibit conformational plasticity, characterized by dynamic and flexible structures, that holds the key to their function.[31–33] The structural plasticity displayed by GPCRs, often modulated by a class of membrane lipids (such as cholesterol),[32] activates various signaling events in response to binding of specific ligands. Activation of GPCRs in response to

Parijat Sarkar

Parijat Sarkar received his Integrated BS–MS degree from Indian Institute of Science Education and Research Kolkata with major in Biological Sciences. He is presently pursuing his PhD at the Centre for Cellular and Molecular Biology, Hyderabad and is a recipient of the S. P. Mukherjee Fellowship. His major interest is in fluorescence spectroscopy, membrane organization, dynamics and lipid–protein interactions. His research also includes monitoring the role of membrane cholesterol in the dynamics and organization of the actin cytoskeleton.

Amitabha Chattopadhyay

Prof. Amitabha Chattopadhyay received B.Sc. with Honors in Chemistry from St. Xavier's College (Calcutta) and M.Sc. in Chemistry from Indian Institute of Technology, Kanpur. He obtained his PhD from the State University of New York at Stony Brook, and was a Postdoctoral Fellow at the University of California, Davis. He subsequently joined the Centre for Cellular and Molecular Biology in Hyderabad, where he is currently a SERB Distinguished Fellow. Prof. Chattopadhyay's work is focused on the role of membrane lipids in the function of G protein-coupled receptors and its implications in health and disease using experimental and simulation approaches. A translational extension of this work has been on the role of host membrane lipids in the entry of intracellular pathogens into host cells. In addition, his group pioneered the development and application of the wavelength-selective fluorescence approach as a novel tool to monitor organization and dynamics of probes and proteins in membranes and micelles. Prof. Chattopadhyay was awarded the prestigious TWAS (The World Academy of Sciences) Prize, Shanti Swarup Bhatnagar Award and Ranbaxy Research Award. He is an elected Fellow of TWAS, the Royal Society of Biology, Royal Society of Chemistry, and all the Indian Academies of Science. He has served on the editorial board of a large number of reputed journals.

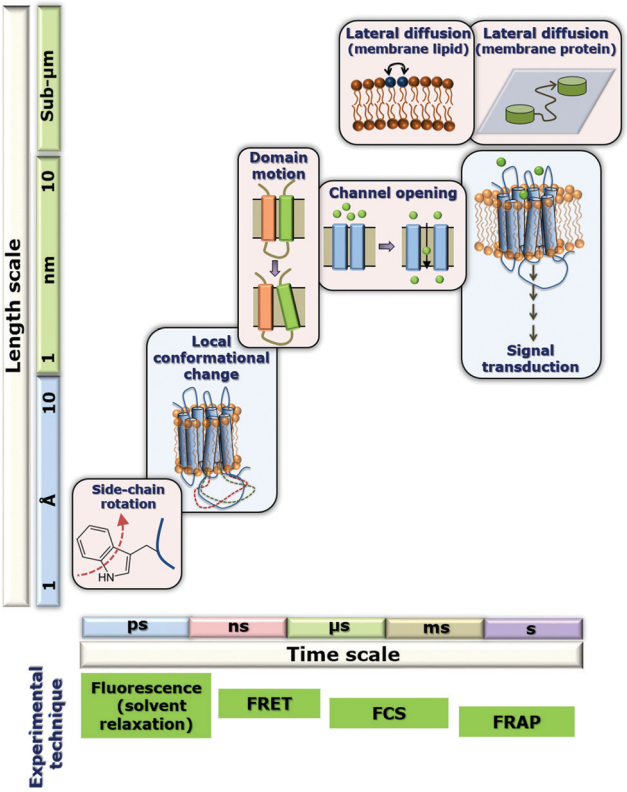

Fig. 1 Diversity of spatiotemporal scales in biomembranes: a schematic map of spatiotemporal dynamics and function of lipids and proteins in membranes. Molecular motions in biological membranes occur over a wide range of spatial and temporal scales. The range of time scales span more than ten orders of magnitude, as apparent from the fact that the amino acid side chain rotations occur in ps time scale, whereas signaling by membrane receptors (such as GPCRs) could take up to a few seconds to minutes. The spatial scale extends over four orders of magnitude, starting from side-chain rotation and up to lateral diffusion of membrane lipids and proteins. Considering the wide range of spatiotemporal scales associated with a gamut of processes in biological membranes, it is not possible to address all membrane phenomena simultaneously using a single experimental technique. Few representative fluorescence-based microscopic and spectroscopic techniques that are sensitive to molecular motions in these time scales are shown at the bottom of the figure. Judicious choice of experimental techniques, appropriate for a corresponding spatiotemporal scale, is crucial for addressing problems related to membrane biology. Adapted and modified from ref. 4 with permission. Copyright 2019 Elsevier Inc.

specific ligands subsequently results in transfer of information inside the cell *via* concerted rearrangement in their transmembrane (or extramembranous) domains.[34] These initial steps of signal transduction, essential for GPCR signaling, take place at the cell membrane through protein–protein interactions. Consequently, receptor dynamics (lateral diffusion) in the plasma membrane determines the overall efficacy of the process of signal transduction.

Diffusion of membrane components represents a fundamental biophysical process that dictates the dynamics of protein–protein and lipid–protein interactions in the membrane.[35,36] Confined lateral diffusion of membrane components often results in compositional heterogeneity (domain) in cell membranes over various time scales. For example, lateral diffusion of lipids and proteins in yeast plasma membrane has been reported to be anomalously slow.[37–42] The relatively slow diffusion of proteins and lipids in yeast membranes is believed to be a plausible reason for maintenance of yeast cell polarity.[38,43] A major reason underlying confined lateral diffusion in biological membranes is the presence of an intricate meshwork of actin cytoskeleton underneath the membrane.[44–47] In this context, the relation between differential mobility of membrane components due to membrane heterogeneity and its effect on modulation of cellular signaling represents an emerging area of research in contemporary biology. The study of lateral mobility (diffusion) of membrane components therefore can be utilized to explore the heterogeneity in membrane organization. Since membrane-bound molecules are characterized by lateral dynamics (diffusion), their functional association with signaling partners largely depends on the probability of their interactions. Cellular signaling originating from the plasma membrane has therefore been hypothesized to be dependent on the mobility of the various interacting components.[48–52] In this overall context, measurement of lateral diffusion of membrane lipids and proteins represents a powerful approach to understand their dynamics in membranes.

4. Membrane dynamics of GPCRs: insight from bleach area dependent FRAP

FRAP is a popular fluorescence microscopy-based approach to measure lateral (translational) diffusion of membrane-bound molecules.[21,25,53–56] In FRAP, a gradient of fluorescent molecules is created by irreversible photobleaching (using high laser power) of a fraction of fluorophores in a small region (typically ~μm dimension) of interest (ROI). The rate of dissipation of this fluorescence gradient, due to diffusion of unbleached fluorophores into the bleached region and bleached fluorophores away from the bleached region, serves as a measure of the lateral diffusion of membrane-bound molecules. Since fluorescence recovery kinetics contains information on the area of the bleach spot, a detailed understanding of spatial organization of membrane-associated molecules could be achieved by varying the ROI dimension (see Fig. 2).[57–60] The lack of invariance in diffusion parameters obtained from FRAP measurements performed with increasing bleach spot size is correlated to the presence of membrane domains of dimensions similar to the bleach spot area.[25,55,59,61–63] The theoretical model based on such interpretation is described below, which was independently validated by FRAP measurements and numerical simulations performed on physically domainized model membranes.[64]

Fluorescence recovery kinetics from FRAP measurements is manifested by two key parameters: an apparent diffusion coefficient (D) and mobile fraction (M_f). D is extracted from the rate of fluorescence recovery of an ensemble of diffraction-limited diffusing molecules, whereas M_f is estimated from the extent of fluorescence recovery within the bleach spot in the time scale of FRAP measurements (typically ~s). In case of

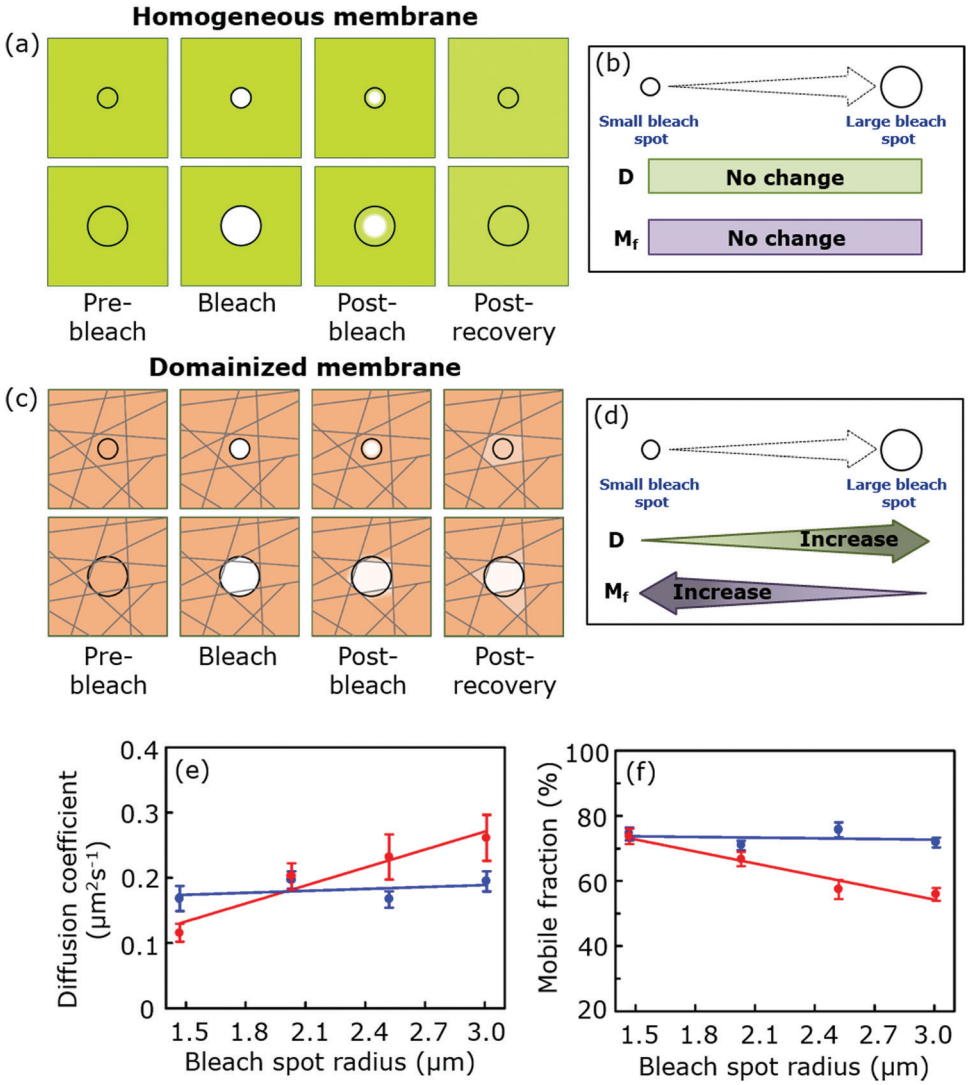

Fig. 2 Effect of membrane heterogeneity on FRAP: fluorescence recovery kinetics of FRAP performed on a homogeneous and domainized membrane with increasing bleach spot area. Conceptual framework of FRAP measurements in (a and b) homogeneous and (c and d) domainized membranes. The homogeneous membrane is characterized by free (random) lateral diffusion throughout the membrane in FRAP time scale. Diffusion parameters (diffusion coefficient (D) and mobile fraction (M_f)) in homogeneous membranes (panel b) remain invariant with increasing bleach spot (provided the bleach spot, indicated by black open circle, is considerably smaller than the total area of the membrane). In contrast, lateral diffusion in domainized membranes is confined to closed areas termed as 'domains' (shown as gray meshwork in panel (c)). These domains are static in the time scale of FRAP and their dimensions are comparable to that of the laser bleach spot. Analysis of FRAP data in domainized membranes yields an apparent D that varies with the size of the bleach spot. This results in an increase in D and decrease in M_f with increasing bleach area (panel (d)). Experimentally observed diffusion parameters from serotonin$_{1A}$-EYFP receptor under control condition (blue) and upon cholesterol depletion (red) using FRAP with bleach spots of varying sizes are shown in panels (e) and (f). The change (lack of invariance) of D and M_f with increasing bleach area is consistent with the dynamic confinement model of the serotonin$_{1A}$ receptor upon cholesterol depletion. Adapted and modified from ref. 60 with permission. Copyright 2007 Elsevier B.V.

lateral diffusion of molecules in a homogeneous membrane (without any domains), the value of D exhibits invariance across all bleach spot radii (Fig. 2a and b). Photobleaching of fluorophores in a small area (top panel in Fig. 2a) results in faster fluorescence recovery, while this recovery is slower in a relatively large bleach area (bottom panel in Fig. 2a), effectively giving rise to constant value of D across all bleach spot sizes (Fig. 2b). In addition, if a significantly smaller area of the plasma membrane (relative to total area of the membrane) is chosen for photobleaching across all bleach spots, fluorescence recovery extents would be similar, resulting in a constant value of M_f (Fig. 2b). However, if molecular diffusion is confined to static (in FRAP time scale) closed domains of dimensions similar to the ROI, diffusion parameters would no longer remain invariant. Under these conditions, bleaching within a small ROI (top panel in Fig. 2c) is likely to report diffusion characteristics of receptors present in these domains, similar to that observed in case of homogeneous membranes. However, a large ROI (exhibiting varying extent of overlap with different domains; see the bottom panel in Fig. 2c) would lead to uneven photobleaching of the domains since bleaching would be complete for a few and partial for others. As a result, fluorescence recovery kinetics across various ROIs would no

longer be proportional to the actual bleach spot size. Since the calculation of D involves the information of bleach spot area, the value of apparent D would show an increase with increasing bleach spot size (Fig. 2d). On the other hand, a large bleach spot would reduce M_f since photobleaching in such a closed domain would result in total loss of receptor fluorescence (Fig. 2d).

5. Dynamic confinement of the serotonin$_{1A}$ receptor upon cholesterol depletion

The serotonin$_{1A}$ receptor[65–67] is a neurotransmitter GPCR that belongs to the subfamily of serotonin receptors.[68] The serotonin$_{1A}$ receptor mediates a multitude of neurological, behavioral and cognitive functions.[69–71] As a consequence of its indispensible role in human physiology, the serotonin$_{1A}$ receptor has emerged as an important drug target in the development of therapeutics against neuropsychiatric disorders (such as anxiety and depression) to even cancer.[72,73] Using a battery of experimental and computational approaches, we have previously reported the requirement of membrane lipids such as cholesterol,[74–78] and sphingolipids[76,79] in the organization, dynamics and function of the serotonin$_{1A}$ receptor.

Several aspects of serotonin$_{1A}$ receptor biology such as cellular organization, trafficking and dynamics are often challenging to address in live cells without a suitable fluorescent tag for optical tracking. For this reason, we previously generated a stable Chinese Hamster Ovary (CHO) cell line heterologously expressing the human serotonin$_{1A}$ receptor tagged to the enhanced yellow fluorescent protein (EYFP; termed serotonin$_{1A}$-EYFP in the rest of the review).[80] We further showed that tagging of the receptor with EYFP could be used to faithfully mimic the native receptor in terms of its pharmacology and cell biology.[80] Fortunately, two-dimensional membrane diffusion coefficient is weakly dependent (logarithmic) on the mass of the diffusing membrane protein (as opposed to diffusion in a bulk solvent).[81] This has served as a boon for FRAP measurements of GFP-tagged membrane proteins, since the mass of the GFP tag ($\sim$26 kDa) itself is substantial relative to typical mass (mol wt) of membrane proteins (*e.g.*, GPCRs are $\sim$50 kDa).[82]

Analysis of FRAP kinetics of serotonin$_{1A}$-EYFP in control cells yielded constant values of D and M_f with respect to increasing bleach spot radius (see blue lines in Fig. 2e and f).[60] Such invariance of D and M_f over a range of bleach spot size implies that the receptor predominantly experiences a homogeneous membrane environment under control conditions. Interestingly, FRAP measurements with an identical range of bleach spot radii performed on cholesterol-depleted cell membranes exhibited a striking dependence of D and M_f of serotonin$_{1A}$ receptors with respect to the bleach spot size (see red lines in Fig. 2e and f). As described above, this type of dependence of D and M_f in cholesterol-depleted membranes is in agreement with a model describing confined diffusion in a domainized membrane.[25,57,59,61–63,83] These observations suggest that cholesterol depletion from cell membranes leads to dynamic confinement of the serotonin$_{1A}$ receptor into confined physical domains that are immiscible in FRAP time scale. These domains restrict diffusion of receptors within their boundaries, resulting in a bleach spot size dependent D and M_f of the receptor. The functional implication of such confinement of receptor dynamics is revealed in signaling carried out by the receptor.[60]

6. Cytoskeleton-induced confined dynamics of the serotonin$_{1A}$ receptor revealed by *z*FCS

The nature of diffusion in biological membranes involves multiple regimes over different spatiotemporal scales. Fluorescence correlation spectroscopy (FCS) offers another sensitive approach for measuring molecular diffusion with increased spatiotemporal resolution.[84,85] In FCS, fluorescence intensity fluctuations due to diffusion of fluorophores in and out of an open confocal volume (typically $\sim$fl dimension) are measured. Unlike FRAP, FCS measurements do not provide any estimate of the immobile molecules since they do not contribute to intensity fluctuations. Information on diffusion coefficient and number of particles in the confocal volume are extracted from the computed autocorrelation function of the fluorescence intensity fluctuations.

However, in case of membrane-bound molecules, commonly used single point FCS measurements often results in inaccurate estimates of diffusion coefficient. This is due to the fact that the axial length ($\sim$1 μm) of FCS observation volume (generated from the diffraction limited illumination of the laser spot) is three orders of magnitude longer than the typical thickness of membrane bilayer ($\sim$5 nm thick).[86] This problem could be circumvented in a variation of the single point FCS measurement, termed as *z*-scanning FCS (*z*FCS). In case of *z*FCS, the uncertainty of positioning the focused laser beam is avoided by a *z*-scan in which the diffusion parameters are determined for a series of *z*-section scans in small increments.[87–90] For Gaussian illumination profiles (represented as positions 1, 2 and 3 in Fig. 3a) and a planar distribution of fluorophores (in this case the serotonin$_{1A}$-EYFP receptor shown as an inset in Fig. 3a) parallel with the focal plane of the microscope, the characteristic diffusion time has a parabolic dependence on the position of the focus (see Fig. 3a). The vertex of the parabola (position 2) is representative of the characteristic diffusion time (τ_D) of the receptor on the membrane. A characteristic plot (see Fig. 3c) of diffusion time (τ_D) *vs.* the transverse area of the confocal volume (Δz^2) generates the "FCS diffusion laws" that provides information on membrane organization at submicron level.[26,91,92] According to FCS diffusion laws, a measure of the nature of diffusion experienced by membrane-bound molecules is obtained from the extrapolated y-intercept to the zero spot size (on y-axis). In case of molecules exhibiting free (random) diffusion (see Fig. 3b), the y-intercept of the linear fit approaches zero, whereas if molecules undergo confined diffusion in the membrane, a negative y-intercept is obtained (see Fig. 3c).

In one of the first applications of this type to GPCRs in live cells, we combined FCS diffusion laws and the principle of *z*FCS.[90]

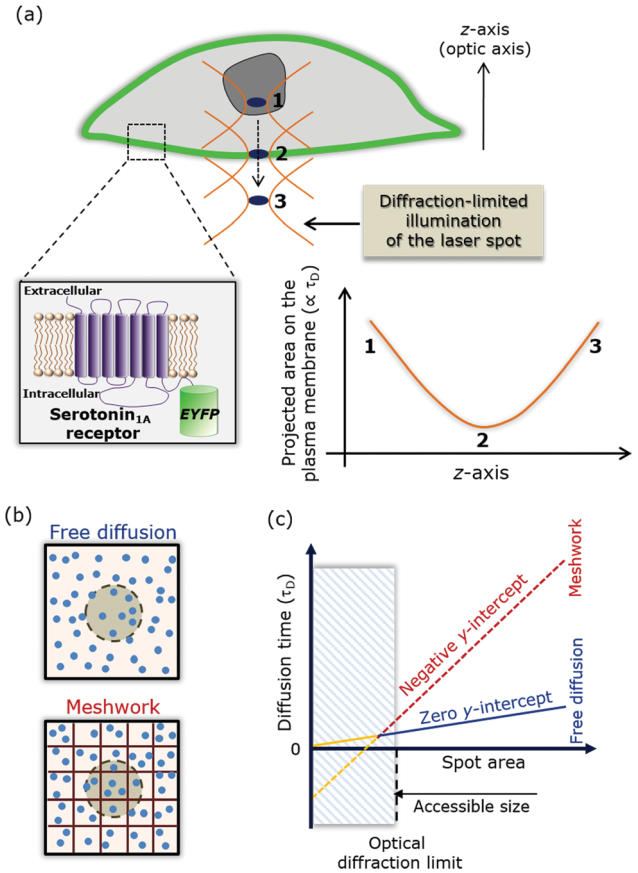

Fig. 3 Principle of *z*-scanning FCS (zFCS) and simulated *z*-FCS diffusion laws for membrane models of varying dynamics. (a) A schematic representation of zFCS. The *z*-axis (or the optic axis, shown by an arrow) is perpendicular to the image plane. The diffraction-limited illumination profile of the laser spot (shown as a blue ellipse) is gradually moved along the *z*-axis (marked by arbitrary positions 1, 2 and 3) resulting in a parabolic scaling of the projected area. A region of interest can therefore be probed at increasing length scales. This allows convenient probing of the plasma membrane (shown as green boundary around the cell) when fluorescence (arising from fluorescently tagged membrane proteins, *e.g.*, the serotonin$_{1A}$ receptor tagged with EYFP in this case) predominantly originates from this region. Because the time taken to diffuse through a circular area should scale with the square of the radius, the characteristic diffusion time (τ_D) for zFCS measurements is related to the projected area illuminated by the diffraction-limited spot on the plane of the plasma membrane. (b) In the free diffusion membrane model, membrane receptors (depicted as blue dots) show pure Brownian (random) motion. In the meshwork model, multiple adjacent domains are separated by barriers such as the mesh of actin cytoskeleton (shown in maroon) under the plasma membrane, preventing free diffusion of molecules. (c) Dependence of diffusion time (τ_D) on the area of observation for free and meshwork membrane models. In a conventional confocal microscope, diffusion law cannot be determined experimentally below the diffraction limit (shown by a dotted line below the *x*-axis). In such a scenario, the extrapolated *y*-intercept to the zero spot size (on the *y*-axis) would provide a measure of the confinement experienced by the diffusing receptor. Adapted and modified from ref. 90 with permission. Copyright 2010 Biophysical Society.

Our results showed that under control condition, the serotonin$_{1A}$ receptor undergoes confined diffusion, as evident from the negative *y*-intercept (~ -21 ms) of the plot of τ_D *vs.* Δz^2 (Fig. 4a). Interestingly, the *y*-intercept value of -21 ms is in agreement with previously reported intercept values for membrane proteins exhibiting confined diffusion induced by the actin cytoskeleton.[92] The estimated diffusion coefficient of the serotonin$_{1A}$ receptor from zFCS measurements was found to be $\sim 4\ \mu m^2\ s^{-1}$. Interestingly, this value of diffusion coefficient is an order of magnitude higher than that obtained using FRAP for the same receptor in same cell type ($\sim 0.14\ \mu m^2\ s^{-1}$, see Fig. 2).[51,60] The apparent mismatch in diffusion coefficient values obtained by FCS and FRAP could be due to the different time scales associated with these techniques (see Fig. 1). Interestingly, the diffusion mode of the serotonin$_{1A}$ receptor remained same in presence of its natural agonist serotonin (Fig. 4b). The *y*-intercept of the plot for serotonin-treated cells was found to be ~ -21 ms, similar to the intercept obtained under control conditions (see Fig. 4a).

What is the cause of confinement of the serotonin$_{1A}$ receptor? This question deserves merit. While the FCS laws are silent about the molecular mechanism underlying the confined nature of the receptor, we exploited dose-dependent (graded) destabilization of the actin cytoskeleton by cytochalasin D (CD), as a tool to obtain insight into the molecular mechanism for receptor confinement. Cytochalasin D is a potent inhibitor of actin polymerization and destabilizes actin by binding to the barbed end of the actin filament which shifts the equilibrium toward depolymerization.[93] Upon treatment of CHO cells expressing serotonin$_{1A}$ receptor with increasing concentrations of CD, receptor confinement was found to be progressively reduced (as evident from a dose-dependent reduction in negative intercept, see Fig. 4c and d).

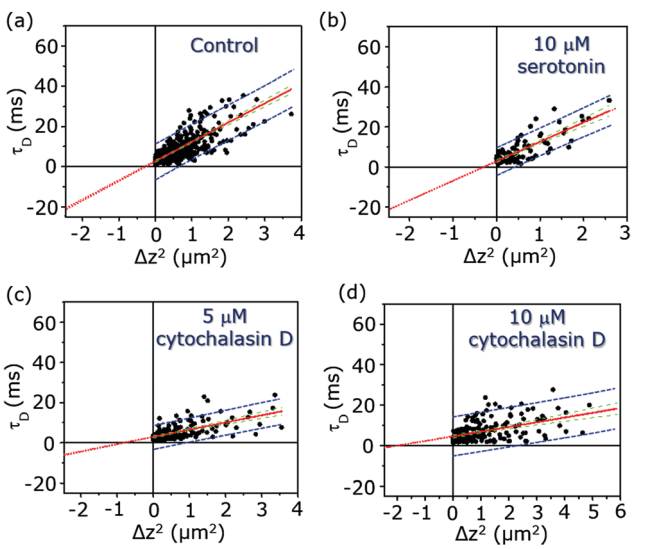

Fig. 4 Monitoring the role of actin cytoskeleton in receptor dynamics using zFCS. The serotonin$_{1A}$ receptor displays confined diffusion, evident from the negative intercept of the plot (panel (a)). (b) Receptor activation by 10 μM serotonin (natural agonist) shows negative intercept of the plot, similar to control cells. Panels (c) and (d) reveal the role of actin cytoskeleton on lateral diffusion. The actin cytoskeleton was destabilized utilizing 5 and 10 μM cytochalasin D, respectively. The progressive release of receptor confinement upon increasing actin destabilization is evident from the dose-dependent increase in the intercept of the plots. The 95% confidence interval (green dashed line) and 95% prediction band (blue dashed line) for the fitted data are also shown. Adapted and modified from ref. 90 with permission. Copyright 2010 Biophysical Society.

This clearly showed that the confinement of the receptor was due to the underlying membrane associated actin cytoskeleton network. This proposition was supported by reduction of the *y*-intercept of the plot from ~−21 ms (control) to ~−5.9 ms in presence of 5 μM CD (see Fig. 4c). In a separate work, we showed that under these conditions ~20% F-actin content was reduced.[94,95] This was further reinforced by a *y*-intercept close to zero (~−1.2 ms) when 10 μM CD was used to depolymerize F-actin (Fig. 4d). These results point out that the combined application of *z*FCS and the FCS diffusion laws could be a powerful strategy to explore membrane heterogeneity at the submicron level.

7. Membrane dynamics at sub-diffraction resolution

As described above, FCS offers a useful handle to explore membrane heterogeneity at sub-μm level by monitoring diffusion modes of proteins and lipids. A more realistic view of biological membranes would emerge by probing membrane heterogeneity at different spatial scales with increasing resolution. However, due to limited spatial resolution of conventional optical microscopy (~250 nm, due to optical diffraction limit), nanoscopic details of such heterogeneity is often overlooked. A possible solution to this limitation is the combination of FCS on a super resolution stimulated emission depletion (STED) microscope.[96–99] In this approach, STED microscopy provides a spatial resolution as low as 50 nm (an order of magnitude higher than conventional confocal microscopes) and allows tuning of the FCS observation spot by changing the power of the STED laser beam.[100] As a consequence, STED-FCS measurements could probe diffusion characteristics at relevant spatial scales.[97,101–103]

A prerequisite for any STED microscopy-based technique is the use of photostable fluorescent probes compatible with stimulated emission depletion. As introduction of fluorescent labels could change properties of lipids, it is important to perform control experiments to rule out any perturbations induced by the fluorescence probe to dynamics of the native lipid. The molecular weight of Atto label (~650 Da) that are generally used in STED-based approaches is in the same range as that of the typical molecular weight of lipids (~700–1000 Da) and therefore could possibly have some influence. In addition, the polarity of the label could change the lipophilic characteristic of the lipid and affect membrane partitioning of the fluorescent lipid analog. It is therefore desirable to perform control experiments using different fluorescent labels to ensure that any perturbation on native lipid dynamics is minimal.

Recently, using fluorescence lifetime correlation spectroscopy (FLCS, an extension of FCS) on a STED microscope, Vicidomini *et al.* reported nanoscale lipid dynamics in plasma membranes of live cells.[104] STED-FLCS is a superior approach to conventional STED-FCS, with improved spatiotemporal resolution and utilizes novel gating strategies based on fluorescence lifetime. Each STED-FLCS measurement allows determination of two important parameters: (a) the apparent diffusion coefficient (D_{max}) using the confocal measurements and (b) the ratio ($D_{ratio} = D_{min}/D_{max}$) of the apparent diffusion coefficients obtained from the smallest observation spot (D_{min}) and the largest observation spot (D_{max}) (see Fig. 5). This ratio (D_{ratio}) is 1 for free diffusion (Fig. 5a and b) when D remains invariant across the entire observation spot. In case of heterogeneous diffusion (*e.g.*, transient trapping due to interaction with immobilized or slowly moving molecules, see Fig. 5a and b), macroscopic diffusion coefficient would always be greater than nanoscopic diffusion coefficient, giving rise to a D_{ratio} value less than 1. For hop diffusion arising due to compartmentalization of membranes by the actin cytoskeleton (Fig. 5a), D_{ratio} value is more than 1 (see Fig. 5b).

Using STED-FLCS measurements, Vicidomini *et al.* explored lipid (phosphatidylethanolamine (PE) and sphingomyelin (SM))

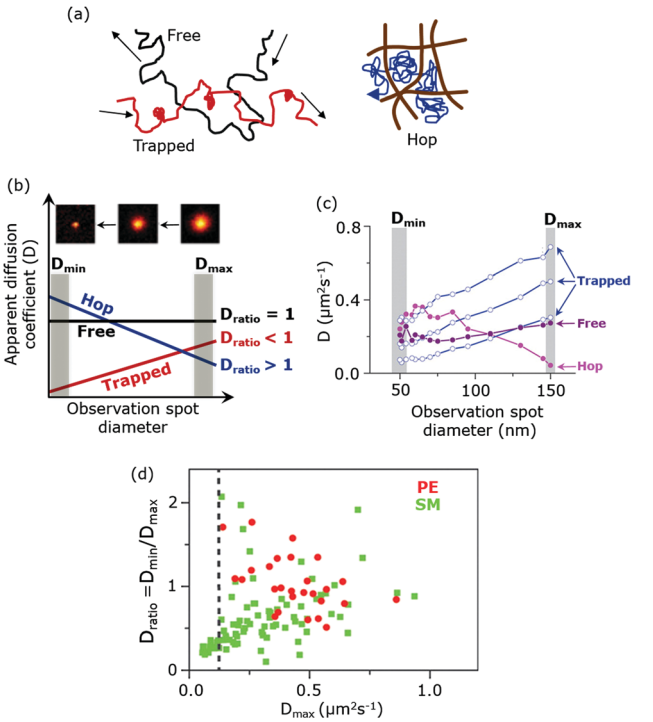

Fig. 5 Theoretical formalism and STED-FLCS measurements. (a) A schematic representation of molecular trajectory for different diffusion modes, such as free diffusion (shown in black), trapped diffusion with transient stops (red) and hop diffusion due to transient compartmentalization (blue, compartments are shown as brown meshwork). (b) Dependence of apparent diffusion coefficient (D) on the observation spot size in different diffusion modes. The useful parameter in STED-FLCS measurement is the ratio D_{ratio}, defined as the ratio of D measured using the smallest (D_{min}) and largest (D_{max}) observation spot. D_{ratio} is 1 for free diffusion, <1 for heterogeneous diffusion due to trapping and >1 for hop diffusion. The top panel in (b) shows typical observation spots of decreasing size (shown by arrow) as formed with increasing STED laser power. (c) Dependence of D on observation spot diameter for 5 representative measurements of sphingomyelin (SM) in Ptk2 cells. The diffusion parameters (D_{max} and D_{min}) are indicated by gray bars. A large heterogeneity in diffusion mode, even for same lipid species, is apparent from the diverse dependence of diffusion coefficient on observation spot diameter (purple, free; blue trapped; magenta, hopping). (d) Scatter plot for D_{max} *vs.* D_{ratio} from STED-FLCS measurements of PE (red) and SM (green) diffusion. The vertical dotted line indicates an arbitrary threshold for strong trapping (D_{max} < 0.14 μm^2 s^{-1}). Adapted and modified from ref. 104 with permission. Copyright 2015 American Chemical Society.

diffusion in plasma membrane of live Ptk2 cells.[104] Unlike model membranes,[105] lipid diffusion in cell membrane could be described by various spatiotemporal models of diffusion (free, trapped and hop; see Fig. 5c). Even for the same lipid species, a large heterogeneity in diffusion modes (free, trapped and hop) could be observed in the plasma membrane (Fig. 5c). This heterogeneity in diffusion modes is highlighted in Fig. 5d. This figure shows a scatter plot of D_{max} and D_{ratio} for the STED-FLCS measurements of PE and SM in plasma membrane of live Ptk2 cells.[104] Both lipids (PE and SM) displayed vast change in diffusion modes, between free (D_{ratio} = 1) and trapped (D_{ratio} < 1) diffusion, but also significant changes in overall macroscopic diffusion (D_{max}) (see Fig. 5d). While the majority of the values for D_{ratio} could be found scattered around 1 for PE, suggesting predominantly free diffusion, SM displayed a more complex and heterogeneous diffusion mode, as apparent from the larger spread of data points. Overall, these results demonstrate the power of STED-FLCS measurements to decipher diffusion modes of relatively small molecules such as membrane lipids in complex biological membranes even below diffraction limit. Such type of analysis in functional biological membranes under various conditions would provide a dynamic map of the membrane which could be relevant in understanding membrane functions at varying spatiotemporal scales.

8. The road ahead

The focus of this perspective is the relevance of varying spatiotemporal scales associated with biological membranes. A nagging question in membrane biology is how to correlate dynamic changes over varying ranges of length and time to integrated membrane function. While a complete solution to this problem is still elusive, we envision that dynamic measurements over varying time and space scales, highlighted in this perspective, could constitute the 'first principles' toward this goal, with continuous advancements in instrumentation and data analysis capability.

Conflicts of interest

There are no conflicts of interest to declare.

Acknowledgements

A. C. gratefully acknowledges support from SERB Distinguished Fellowship (Department of Science and Technology, Govt. of India). P. S. thanks the Council of Scientific and Industrial Research for the award of a Shyama Prasad Mukherjee Fellowship. A. C. is a Distinguished Visiting Professor at the Indian Institute of Technology Bombay (Mumbai), and Adjunct Professor at the RMIT University (Melbourne, Australia), Tata Institute of Fundamental Research (Mumbai) and Indian Institute of Science Education and Research (Kolkata), and an Honorary Professor at the Jawaharlal Nehru Centre for Advanced Scientific Research (Bengaluru). Some of the work described in this article was carried out by former members of A. C.'s research group whose contributions are gratefully acknowledged. We thank members of the Chattopadhyay laboratory for comments and discussions.

References

1 S. Pal and A. Chattopadhyay, in *Membrane organization and dynamics*, ed. A. Chattopadhyay, Springer, Heidelberg, 2017, pp. 1–9.
2 K. Jacobson, O. G. Mouritsen and R. G. W. Anderson, *Nat. Cell Biol.*, 2007, **9**, 7–14.
3 E. Sezgin, I. Levental, S. Mayor and C. Eggeling, *Nat. Rev. Mol. Cell Biol.*, 2017, **18**, 361–374.
4 P. Sarkar, G. A. Kumar, S. Pal and A. Chattopadhyay, in *Serotonin: the mediator that spans evolution*, ed. P. Pilowsky, Elsevier, Amsterdam, 2018, pp. 3–22.
5 K. Simons and D. Toomre, *Nat. Rev. Mol. Cell Biol.*, 2000, **1**, 31–39.
6 K. L. Pierce, R. T. Premont and R. J. Lefkowitz, *Nat. Rev. Mol. Cell Biol.*, 2002, **3**, 639–650.
7 D. M. Rosenbaum, S. G. F. Rasmussen and B. K. Kobilka, *Nature*, 2009, **459**, 356–363.
8 K. Palczewski and T. Orban, *Annu. Rev. Neurosci.*, 2013, **36**, 139–164.
9 A. Chattopadhyay, *Adv. Biol.*, 2014, 143023.
10 Y. Zhang, M. E. DeVries and J. Skolnick, *PLoS Comput. Biol.*, 2006, **2**, e13.
11 M. Audet and M. Bouvier, *Nat. Chem. Biol.*, 2008, **4**, 397–403.
12 D. Hilger, M. Masureel and B. K. Kobilka, *Nat. Struct. Mol. Biol.*, 2018, **25**, 4–12.
13 B. Bosier and E. Hermans, *Trends Pharmacol. Sci.*, 2007, **28**, 438–446.
14 R. M. Cooke, A. J. H. Brown, F. H. Marshall and J. S. Mason, *Drug Discovery Today*, 2015, **20**, 1355–1364.
15 K. A. Jacobson, *Biochem. Pharmacol.*, 2015, **98**, 541–555.
16 A. S. Hauser, M. M. Attwood, M. Rask-Andersen, H. B. Schiöth and D. E. Gloriam, *Nat. Rev. Drug Discovery*, 2017, **16**, 829–842.
17 K. Sriram and P. A. Insel, *Mol. Pharmacol.*, 2018, **93**, 251–258.
18 H. C. S. Chan, Y. Li, T. Dahoun, H. Vogel and S. Yuan, *Trends Biochem. Sci.*, 2019, **44**, 312–330.
19 J.-J. Lacapère, E. Pebay-Peyroula, J.-M. Neumann and C. Etchebest, *Trends Biochem. Sci.*, 2007, **32**, 259–270.
20 D. Sengupta, G. A. Kumar, X. Prasanna and A. Chattopadhyay, in *Computational biophysics of membrane proteins*, ed. C. Domene, Royal Society of Chemistry, London, 2017, pp. 137–160.
21 J. Lippincott-Schwartz, E. Snapp and A. Kenworthy, *Nat. Rev. Mol. Cell Biol.*, 2001, **2**, 444–456.
22 M. Jafurulla and A. Chattopadhyay, in *Springer series on fluorescence*, ed. Y. Mely and G. Duportail, Springer, Heidelberg, 2013, **13**, pp. 417–437.
23 A. Chattopadhyay and S. Haldar, *Acc. Chem. Res.*, 2014, **47**, 12–19.
24 H. Chakraborty and A. Chattopadhyay, *ACS Chem. Neurosci.*, 2015, **6**, 199–206.

25 A. Chattopadhyay and M. Jafurulla, *Adv. Exp. Med. Biol.*, 2015, **842**, 27–40.
26 H.-T. He and D. Marguet, *Annu. Rev. Phys. Chem.*, 2011, **62**, 417–436.
27 N. Bag, S. Huang and T. Wohland, in *Membrane organization and dynamics*, ed. A. Chattopadhyay, Springer, Heidelberg, 2017, pp. 113–145.
28 R. Nygaard, Y. Zou, R. O. Dror, T. J. Mildorf, D. H. Arlow, A. Manglik, A. C. Pan, C. W. Liu, J. J. Fung, M. P. Bokoch, F. S. Thian, T. S. Kobilka, D. E. Shaw, L. Mueller, R. S. Prosser and B. K. Kobilka, *Cell*, 2013, **152**, 532–542.
29 A. Manglik, T. H. Kim, M. Masureel, C. Altenbach, Z. Yang, D. Hilger, M. T. Lerch, T. S. Kobilka, F. S. Thian, W. L. Hubbell, R. S. Prosser and B. K. Kobilka, *Cell*, 2015, **161**, 1101–1111.
30 P. Schmidt, L. Thomas, P. Müller, H. A. Scheidt and D. Huster, *Chemistry*, 2014, **20**, 4986–4992.
31 X. Deupi, C. Govaerts, L. Shi, J. A. Javitch, L. Pardo and J. Ballesteros, in *Contemporary clinical neuroscience: the G protein-coupled receptors handbook*, ed. L. A. Devi, Humana Press Inc., Totowa, New Jersey, 2005, pp. 363–388.
32 X. Prasanna, D. Sengupta and A. Chattopadhyay, *Sci. Rep.*, 2016, **6**, 31858.
33 N. R. Latorraca, A. J. Venkatakrishnan and R. O. Dror, *Chem. Rev.*, 2017, **117**, 139–155.
34 W. I. Weis and B. K. Kobilka, *Annu. Rev. Biochem.*, 2018, **87**, 897–919.
35 M. Edidin, *Curr. Top. Membr.*, 1996, **43**, 1–13.
36 F. Oswald, E. L. M. Bank, Y. J. M. Bollenac and E. J. G. Peterman, *Phys. Chem. Chem. Phys.*, 2014, **16**, 12625–12634.
37 M. L. Greenberg and D. Axelrod, *J. Membr. Biol.*, 1993, **131**, 115–127.
38 J. Valdez-Taubas and H. R. B. Pelham, *Curr. Biol.*, 2003, **13**, 1636–1640.
39 K. Mukhopadhyay, T. Prasad, P. Saini, T. J. Pucadyil, A. Chattopadhyay and R. Prasad, *Antimicrob. Agents Chemother.*, 2004, **48**, 1778–1787.
40 S. Ganguly, P. Singh, R. Manoharlal, R. Prasad and A. Chattopadhyay, *Biochem. Biophys. Res. Commun.*, 2009, **387**, 661–665.
41 N. K. Khandelwal, P. Sarkar, N. A. Gaur, A. Chattopadhyay and R. Prasad, *Biochim. Biophys. Acta*, 2018, **1860**, 2308–2319.
42 N. K. Khandelwal, N. Chauhan, P. Sarkar, B. D. Esquivel, P. Coccetti, A. Singh, A. T. Coste, M. Gupta, D. Sanglard, T. C. White, M. Chauvel, C. d'Enfert, A. Chattopadhyay, N. A. Gaur, A. K. Mondal and R. Prasad, *J. Biol. Chem.*, 2018, **293**, 412–432.
43 B. D. Slaughter, J. R. Unruh, A. Das, S. E. Smith, B. Rubinstein and R. Li, *Nat. Commun.*, 2013, **4**, 1380.
44 T. Fujiwara, K. Ritchie, H. Murakoshi, K. Jacobson and A. Kusumi, *J. Cell Biol.*, 2002, **157**, 1071–1081.
45 A. Kusumi, H. Murakoshi, K. Murase and T. Fujiwara, in *Biophysical aspects of transmembrane signaling (Springer series in biophysics)*, ed. S. Damjanovich, Springer-Verlag, Berlin, 2005, pp. 123–152.
46 D. M. Andrade, M. P. Clausen, J. Keller, V. Mueller, C. Wu, J. E. Bear, S. W. Hell, B. C. Lagerholm and C. Eggeling, *Sci. Rep.*, 2015, **5**, 11454.
47 M. Fritzsche, D. Li, H. Colin-York, V. T. Chang, E. Moeendarbary, J. H. Felce, E. Sezgin, G. Charras, E. Betzig and C. Eggeling, *Nat. Commun.*, 2017, **8**, 14347.
48 R. Peters, *FEBS Lett.*, 1988, **234**, 1–7.
49 D. A. Jans, R. Peters, J. Zsigo and F. Fahrenholz, *EMBO J.*, 1989, **8**, 2481–2488.
50 P. D. Calvert, V. I. Govardovskii, N. Krasnoperova, R. E. Anderson, J. Lem and C. L. Makino, *Nature*, 2001, **411**, 90–94.
51 S. Ganguly, T. J. Pucadyil and A. Chattopadhyay, *Biophys. J.*, 2008, **95**, 451–463.
52 A. J. B. Kreutzberger, M. Ji, J. Aaron, L. Mihaljević and S. Urban, *Science*, 2019, **363**, eaao0076.
53 M. Edidin, in *Mobility and proximity in biological membranes*, ed. S. Damjanovich, J. Szöiiósi, L. Trón and M. Edidin, CRC, Boca Raton, Florida, 1994, pp. 109–135.
54 N. Klonis, M. Rug, I. Harper, M. Wickham, A. Cowman and L. Tilley, *Eur. Biophys. J.*, 2002, **31**, 36–51.
55 G. M. Hagen, D. A. Roess, G. C. de León and B. G. Barisas, *J. Fluoresc.*, 2005, **15**, 873–882.
56 B. C. Lagerholm, G. E. Weinreb, K. Jacobson and N. L. Thompson, *Annu. Rev. Phys. Chem.*, 2005, **56**, 309–336.
57 M. Edidin and I. Stroynowski, *J. Cell Biol.*, 1991, **112**, 1143–1150.
58 Y. I. Henis, B. Rotblat and Y. Kloog, *Methods*, 2006, **40**, 183–190.
59 L. Cézanne, S. Lecat, B. Lagane, C. Millot, J.-Y. Vollmer, H. Matthes, J.-L. Galzi and A. Lopez, *J. Biol. Chem.*, 2004, **279**, 45057–45067.
60 T. J. Pucadyil and A. Chattopadhyay, *Biochim. Biophys. Acta*, 2007, **1768**, 655–668.
61 E. Yechiel and M. Edidin, *J. Cell Biol.*, 1987, **105**, 755–760.
62 A.-M. Baker, A. Saulière, G. Gaibelet, B. Lagane, S. Mazères, M. Fourage, F. Bachelerie, L. Salomé, A. Lopez and F. Dumas, *J. Biol. Chem.*, 2007, **282**, 35163–35168.
63 A. N. Saulière-Nzeh, C. Millot, M. Corbani, S. Mazères, A. Lopez and L. Salomé, *J. Biol. Chem.*, 2010, **285**, 14514–14520.
64 L. Salomé, J.-L. Cazeils, A. Lopez and J.-F. Tocanne, *Eur. Biophys. J.*, 1998, **27**, 391–402.
65 T. J. Pucadyil, S. Kalipatnapu and A. Chattopadhyay, *Cell. Mol. Neurobiol.*, 2005, **25**, 553–580.
66 S. Kalipatnapu and A. Chattopadhyay, *Cell. Mol. Neurobiol.*, 2007, **27**, 1097–1116.
67 C. P. Müller, R. J. Carey, J. P. Huston and M. A. De Souza Silva, *Prog. Neurobiol.*, 2007, **81**, 133–178.
68 D. E. Nichols and C. D. Nichols, *Chem. Rev.*, 2008, **108**, 1614–1641.
69 J. A. Gordon and R. Hen, *NeuroMol. Med.*, 2004, **5**, 27–40.
70 R. H. Belmaker and G. Agam, *N. Engl. J. Med.*, 2008, **358**, 55–68.
71 J. Kaufman, C. DeLorenzo, S. Choudhury and R. V. Parsey, *Eur. Neuropsychopharmacol.*, 2016, **26**, 397–410.
72 E. Lacivita, M. Leopoldo, F. Berardi and R. Perrone, *Curr. Top. Med. Chem.*, 2008, **8**, 1024–1034.
73 F. Fiorino, B. Severino, E. Magli, A. Ciano, G. Caliendo, V. Santagada, F. Frecentese and E. Perissutti, *J. Med. Chem.*, 2014, **57**, 4407–4426.

74 T. J. Pucadyil and A. Chattopadhyay, *Prog. Lipid Res.*, 2006, **45**, 295–333.
75 Y. D. Paila and A. Chattopadhyay, *Subcell. Biochem.*, 2010, **51**, 439–466.
76 M. Jafurulla and A. Chattopadhyay, *Curr. Med. Chem.*, 2013, **20**, 47–55.
77 D. Sengupta and A. Chattopadhyay, *Biochim. Biophys. Acta*, 2015, **1848**, 1775–1782.
78 D. Sengupta, X. Prasanna, M. Mohole and A. Chattopadhyay, *J. Phys. Chem. B*, 2018, **122**, 5727–5737.
79 M. Jafurulla and A. Chattopadhyay, *Eur. J. Pharmacol.*, 2015, **763**, 241–246.
80 T. J. Pucadyil, S. Kalipatnapu, K. G. Harikumar, N. Rangaraj, S. S. Karnik and A. Chattopadhyay, *Biochemistry*, 2004, **43**, 15852–15862.
81 P. G. Saffman and M. Delbrück, *Proc. Natl. Acad. Sci. U. S. A.*, 1975, **72**, 3111–3113.
82 P. Sarkar and A. Chattopadhyay, *J. Biosci.*, 2018, **43**, 421–430.
83 R. Saxena and A. Chattopadhyay, *J. Neurochem.*, 2011, **116**, 726–733.
84 E. Haustein and P. Schwille, *Annu. Rev. Biophys. Biomol. Struct.*, 2007, **36**, 151–169.
85 E. L. Elson, *Biophys. J.*, 2011, **101**, 2855–2870.
86 S. T. Hess, S. Huang, A. A. Heikal and W. W. Webb, *Biochemistry*, 2002, **41**, 697–705.
87 A. Benda, M. Beneš, V. Mareček, A. Lhotsky, W. T. Hermens and M. Hof, *Langmuir*, 2003, **19**, 4120–4126.
88 J. Humpolíčková, E. Gielen, A. Benda, V. Fagulova, J. Vercammen, M. vandeVen, M. Hof, M. Ameloot and Y. Engelborghs, *Biophys. J.*, 2006, **91**, L23–L25.
89 J. Ries and P. Schwille, *Phys. Chem. Chem. Phys.*, 2008, **10**, 3487–3497.
90 S. Ganguly and A. Chattopadhyay, *Biophys. J.*, 2010, **99**, 1397–1407.
91 L. Wawrezinieck, H. Rigneault, D. Marguet and P.-F. Lenne, *Biophys. J.*, 2005, **89**, 4029–4042.
92 P.-F. Lenne, L. Wawrezinieck, F. Conchonaud, O. Wurtz, A. Boned, X.-J. Guo, H. Rigneault, H.-T. He and D. Marguet, *EMBO J.*, 2006, **25**, 3245–3256.
93 P. Sampath and T. D. Pollard, *Biochemistry*, 1991, **30**, 1973–1980.
94 S. Ganguly, R. Saxena and A. Chattopadhyay, *Biochim. Biophys. Acta*, 2011, **1808**, 1921–1929.
95 S. Roy, G. A. Kumar, M. Jafurulla, C. Mandal and A. Chattopadhyay, *Biochim. Biophys. Acta*, 2014, **1838**, 2011–2018.
96 L. Kastrup, H. Blom, C. Eggeling and S. W. Hell, *Phys. Rev. Lett.*, 2005, **94**, 178104.
97 C. Eggeling, C. Ringemann, R. Medda, G. Schwarzmann, K. Sandhoff, S. Polyakova, V. N. Belov, B. Hein, C. von Middendorff, A. Schönle and S. W. Hell, *Nature*, 2009, **457**, 1159–1162.
98 S. J. Sahl, M. Leutenegger, M. Hilbert, S. W. Hell and C. Eggeling, *Proc. Natl. Acad. Sci. U. S. A.*, 2010, **107**, 6829–6834.
99 C. Roobala, I. P. Ilanila and J. K. Basu, *J. Biosci.*, 2018, **43**, 471–484.
100 L. Schermelleh, A. Ferrand, T. Huser, C. Eggeling, M. Sauer, O. Biehlmaier and G. P. C. Drummen, *Nat. Cell Biol.*, 2019, **21**, 72–84.
101 V. Mueller, C. Ringemann, A. Honigmann, G. Schwarzmann, R. Medda, M. Leutenegger, S. Polyakova, V. N. Belov, S. W. Hell and C. Eggeling, *Biophys. J.*, 2011, **101**, 1651–1660.
102 A. Honigmann, V. Mueller, H. Ta, A. Schoenle, E. Sezgin, S. W. Hell and C. Eggeling, *Nat. Commun.*, 2014, **5**, 5412.
103 N. K. Sarangi, K. G. Ayappa, S. S. Visweswariah and J. K. Basu, *Phys. Chem. Chem. Phys.*, 2016, **18**, 29935–29945.
104 G. Vicidomini, H. Ta, A. Honigmann, V. Mueller, M. P. Clausen, D. Waithe, S. Galiani, E. Sezgin, A. Diaspro, S. W. Hell and C. Eggeling, *Nano Lett.*, 2015, **15**, 5912–5918.
105 M. P. Clausen, E. Sezgin, J. B. de la Serna, D. Waithe, B. C. Lagerholm and C. Eggeling, *Methods*, 2015, **88**, 67–75.